Structures and Architecture. REstructure REmaterialize REthink REuse - Rinke & Frier Hvejsel (Eds)
© 2025 The Author(s), ISBN 978-1-041-11139-9
Open Access: www.taylorfrancis.com, CC BY-NC-ND 4.0 license

Towards automating the workflow for design, manufacturing, and assembly process feedback of discrete panel structures

S. Wilcock & O. Iuorio
Politecnico di Milano, Italy

ABSTRACT: While computer aided design software allows for rapid exploration of architectural forms, transferring these designs to machinery for digital fabrication and assembly processes is often manual. This paper outlines steps to automate digital fabrication and monitor assembly processes for thin structural panels, aiming to integrate these tools into the designer's workflow. Much of the current state of the art focuses on unidirectional data flow from design to manufacture, with little capability for process monitoring in assembly. In this work, laser cutting has been utilised with a stacked contour technique, to realise complex 3D geometries from planar sheets at low-cost, and the methods for automating slicing and placement of reference dowels are described. With regards to assembly, panels are designed to be handled by a robot manipulator arm using readily sourced timber dowels and custom robot end-effectors; towards this end, a bidirectional connection between design software and sensor data is described, and results are presented on experiments with Apriltag fiducial tags cut into wood with which to get process feedback through cameras. Using this sensor data, panel poses can be estimated, and results on Apriltag pose feedback with a set of test panels are reported. A prototype of a thin dry stacked panel structure has been developed and assembled as a case study into the manufacture process, and to demonstrate the adaptive robotic planning opportunity provided in integrating live sensor data into parametric CAD software. As-designed panel poses are compared to real pose data, and additionally to pointcloud data suggesting space for further development. Through these integrations into the design process, this research aims to contribute to the capabilities of the architecture engineering and construction (AEC) sector, to streamline the use of modern fabrication and robotics hardware for disassemblable systems.

1 INTRODUCTION

Digital fabrication has revolutionized architectural design, enabling rapid exploration of complex forms through computer-aided design (CAD) software. However, the transition from digital models to physical fabrication and assembly remains predominantly manual, leading to inefficiencies and limitations in rapid prototyping. Current workflows often exhibit a unidirectional data flow from design to manufacturing, lacking feedback mechanisms for monitoring assembly processes, which can hinder design iterations and adaptability. Particularly in the use of robotics hardware, most parametric design solutions such as Kuka—PRC and HAL (Braumann, 2019) are offline planners, which cannot adapt or accept ongoing process feedback.

To address these challenges, this paper outlines a comprehensive approach to automating the workflow of design, manufacture, and assembly for shell structure panels. The proposed method leverages laser cutting with a stacked contour technique to facilitate the realization of intricate 3D geometries from planar sheets. Using packing algorithms (Vestartas, 2021), it is possible to reduce material waste in laser cutting by attempting to optimise cutting shape placement within the available material stock.

The integration of sensor technologies, such as low-cost cameras for process feedback, further enhances this automated workflow. By employing fiducial markers, such as the QR code styled

DOI: 10.1201/9781003658641-58

Apriltags, the robotic system can gain valuable insights into panel positioning and orientation, enabling precise adjustments during assembly (Iturralde et al., 2023). This level of feedback is crucial for maintaining the alignment and integrity of structures during assembly, where minor discrepancies can significantly impact particularly robotic assembly success, whilst flexible materials and deflections might be another target for using fiducial tags (Song et al., 2021). While these features can be readily implemented in robotics middleware such as ROS (Quigley et al., 2009), it is not as accessible to the architectural designer as integrated CAD capabilities. The Falcon software package had some fiducial tag capabilities integrated into Grasshopper, but they did not have access to live data feeds, and the plugin is now defunct (Chen, 2016).

By automating the workflow of design, manufacture, and assembly for shell structure panels, this research aims to bridge gaps and enhance the capabilities of the architectural designer in using robotic technologies. Through the integration of algorithmic design, laser cutting, and real-time feedback mechanisms, this work seeks to streamline the design transfer process, promote rapid iteration in architectural prototyping, and ultimately contribute to the development of disassemblable systems that align with the evolving demands for sustainability and efficiency in construction practices (Iuorio et al., 2024; Tafazzoli, 2022).

2 METHODOLOGY

2.1 *Structure design and digital fabrication workflow*

The aim of the project was to use timber material to construct a thin panel structure as a test bed for robotic assembly, with the intention of being dry stacked such that it could be disassembled with ease. In the authors' recent work, a design process and set of structural analysis tools was developed to create such structures which are dominated by membrane forces once fully assembled and are thus inherently stable, yet which can support themselves with cantilevering action during assembly wilcockIntegratingRfunicularityLocal2024. A full scale model of height 2m and 1.8x1.8m span was designed to align with the appropriate reach space of the available robotic manipulator. Dovetail joints support the structure during assembly, however are limited to positive Gaussian curvature designs. Figure 1 shows the full structural design, with a highlighted subset of panels selected for manufacture.

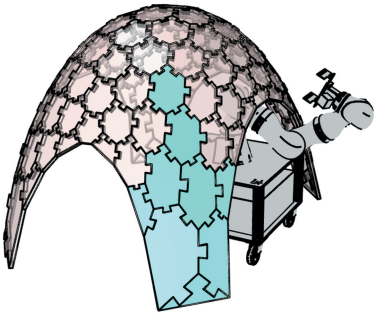

Figure 1. The designed self supporting shell, with highlighted section showing the selected test panels for manufacture. The robot arm has an Apriltag on each corner, for camera recognition of where the arm is in relation to panels.

To slice the panels into curves which the laser cutter can read, first the panel internal faces, or intrados, are found by searching for the largest two faces for each panel, and finding the distance to the shell centre point – the lesser of the two distances is the intrados. Since the panel intrados and extrados are planar, it is trivial to fit a plane to them. Having done this, a naïve method of finding the minimal bounding box is implemented and the panels are reoriented to the XY plane.

Once the panel layers are cut, it is desirable to have reference dowels inserted into the stack to ensure that layers are correctly aligned with one another. In order to find the best location and the largest possible distance to place rods, which can also have a design etched into the centre for robotic assembly later, inspiration is taken from the field of geography. Poles of inaccessibility is a term usually used to describe remote locations on Earth which are the furthest point from any coastline, that may be considered a visual centre point (Garcia-Castellanos and Lombardo, 2007), and lends itself well to this problem where we have defined boundary curves given by the bottom face of the panels. Techniques for finding these locations generally involve an adaptive search grid, however a reasonable approach for the current problem does not necessarily require adaptive iteration (Algorithm 1).

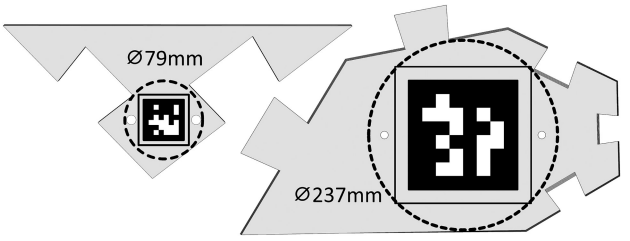

Figure 2. Two panels from the section base showing the internal faces, with a dotted line marking the largest circle possible about the pole of inaccessibility. Finding these centrepoints allows the largest possible Apriltags and spacing of dowel rods.

Algorithm 1 Finding the pole of inaccessibility within a panel boundary curve, taking a panel outline curve as input.

```
Input: panelOutline (Crv), nDivisions (Int)
Output: bestPoint (Pnt), bestRadius (Float)
    Initialisation:
 1: bBox = panel.getBoundingBox()
 2: bestRadius = -1
    LOOP
 3: for x = bBox.xMin + i/bBox.xRange, i = 1 to nDivisions do
 4:    for y = bBox.yMin + i/bBox.yRange, i = 1 to nDivisions do
 5:       testPt = Point(x, y)
 6:       if NOT panelOutline.Contains(testPt) then
 7:          continue
 8:       end if
 9:       ptOnCrv = panelOutline.getClosestPoint(testPt)
10:       dist = ptOnCrv – testPt
11:       if dist.Length > bestRadius then
12:          bestRadius = dist.Length
13:          bestPoint = testPt
14:       end if
15:    end for
16: end for
17: return bestPoint, bestRadius
```

This algorithm was scripted as a Grasshopper component in C# and gives locations for the reference dowels which are guaranteed to be a) within the bounds of the surface, and b) scaled to the empty space on the panel. Additionally, this allows for larger Apriltag codes to be added (Figure 3) providing better resolution images for pose estimation later, giving

results shown in Figure 2. It should also be noted, that due to the minimal bounding box alignment, the dowels additionally end up aligned to the longest bounded length of the panels.

Taking these reoriented panels with reference holes, it is now required to manufacture the part. Initially, CNC milling was considered for fabricating the parts, however due to the panel design relying on a mixture of edge chamfer directions, 5 axis CNC would be required, and quotes were higher than the laser cutting cost by a factor of 20x. Slicing the panels was relatively simple; contours were generated by intersecting planes with the panels at heights h=0, t, 2t, 3t... etc. for sheet material values of t (Figure 3). Contours were additionally offset outwards by 1mm, to compensate for the kerf formed by the width of the laser beam.

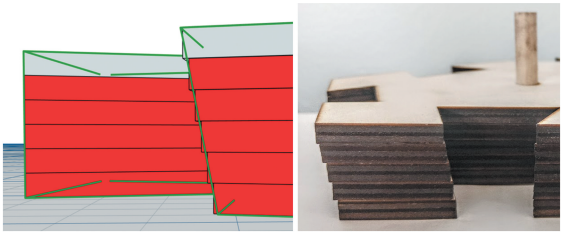

Figure 3. Slicing discretization of the panels. Left: With wireframe overlay; Right: Prototype.

Using OpenNest (Vestartas, 2021) it is possible to generate packings of boundary curves which are extremely tight, helping designers achieve optimal material utilization. Additionally, as with the other aspects of the digital fabrication workflow, OpenNest can be used automatically, adjusting its output with any parametric change in the structure. The curves were assigned colours depending on their requirements (here in Figure 4 – blue for etching, red for cutting, and black for rastering, i.e. burning large areas), before automatic export to DXF vector drawing files which the laser cutter can read. Using such an automated workflow directly linked to the CAD software allows rapid generation of fabrication definitions. The sheet in Figure 4 took 15 minutes to cut, with the majority of time spent rastering the black Apriltag regions, and for the entire test set of 6 panels, each of 6 layers, it took only 3 hours 20 minutes and 13 sheets to manufacture. Having cut the panels, they were stacked and glued with PVA, and dowel rods inserted (Figure 4). Some minor post processing was required, namely some light sanding to remove the step edges shown in Figure 3.

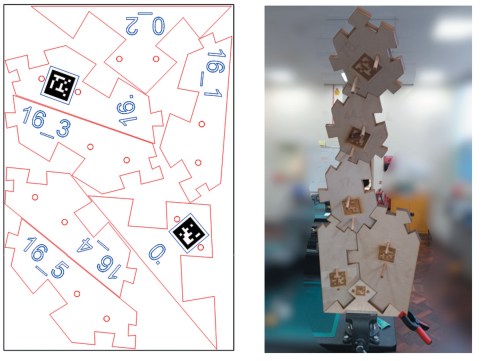

Figure 4. Left: Laser cutting layout of a 400x600mm sheet populated with test panels, generated using OpenNest. Right: The cut and glued panels assembled. Some Apriltags were reduced in size to accommodate the limited grasp width of the robot end effector.

2.2 *Sensing of panels for process feedback*

A custom Python 3 module was written to deal with a number of aspects: primarily, the flow of camera data into Grasshopper; the recognition of Apriltags and their pose estimation; bundle recognition and pose estimation; and the flow of colour registered pointcloud data from the camera to Grasshopper.

For accurate estimation of panel poses based on the location of their fiduciary tags within the camera image, a number of calibration and configuration steps first had to be carried out. The camera was calibrated at a distance of 3m using a large checkerboard, in order to gain the camera's distortion and intrinsic matrices, respectively for combating distortion and to translate from points in the camera space to points in 3D space. The panel meshes, Apriltag sizes and orientation were exported to a JSON format file for easy reading, as were the relative locations of the paper bundle's tags. Based on earlier works (Malyuta, 2017, 2018), the perspective-n-point (PNP) algorithm (Fischler and Bolles, 1981) was utilised through OpenCV (Bradski, 2000) to recognise the base point of bundles within the camera's field of view using all of the visible tags. This allows the bundle to be recognised with partial occlusion, i.e. when some or even most of the bundle's tags are obstructed from the camera.

In order to measure the difference between a pose estimate and the ground truth values, it would be possible to simply take distance measurements from the base points of the panels. This does not however take into account the rotation of panels; for this, the average distance metric ADD-6d (Hinterstoisser et al., 2013) is used:

$$ADD^p = \frac{1}{M}\sum_j \min_{0<k<M} \parallel (Rx_j + t) - (\bar{R}x_k + \bar{t}) \parallel \quad (1)$$

where pose $p = R|t$ is the ground truth pose, made up of a rotation matrix R and a column vector of translations t, and similarly $\bar{p} = \bar{R}|\bar{t}$ is the pose estimate. M is the number of points in the test set. The ADD-6d metric is fundamentally finding the average distance error between each pose point on the panel mesh and its closest counterpart point, for which we populated the mesh geometry with 10x10x10 points. This allows us to compare poses given by Apriltags both to expected poses by using a single panel as a reference upon which we use the transformation frames between neighbours as-designed, and to pointcloud data with which we can refine the knowledge of the assembly scene state.

With careful processing of transformation frames using custom nodes, it is also possible to align the different transformation frames providing live feedback on a construction scene, allowing the user to follow the assembly process, and feasibly to provide recommendations for adaptive assembly patterns in the case of less bespoke, reconfigurable structural elements.

2.3 *Experimental setup*

In order to assess and monitor the assembly process for the panel system, an Orbbec Astra 640x480px depth camera and tripod was set up. To simulate the use of a robot base with a bundle of markers for registration, an A4 sheet of 4 Apriltag 36h11 markers was printed with known spacing and placed in the camera's field of view. 3 interlocking panels were selected for experimentation, numbered 21, 28 and 48. A series of tests were devised to demonstrate and measure the capabilities of the system.

For testing the capabilities of the tag pose measurement and additionally the tag bundle suitability, test panel #21 was first placed level with the bundle, before being raised in 30° increments using an adjustable protractor (Figure 5(a)-5(d)). Both ADD were used (comparing to pointcloud data) and angle measurements of the panel using the fiduciary tag data. An additional two tests were devised to test adding panels into the system (panels #28 and #48), where in addition to pointcloud data, panel #21 was used as a reference pose by which to compare the relative placement of panels to the design intent (Figure 5(e)-5(g)). Finally, without the tag bundle in place, a further 3 tests were set using a misaligned pair of panels (#28 and #48) (Figure 5(g)-5(i)). The misalignment was fixed, however the distance to the panels and camera orientation was altered to test the effect of angle, lighting and distance.

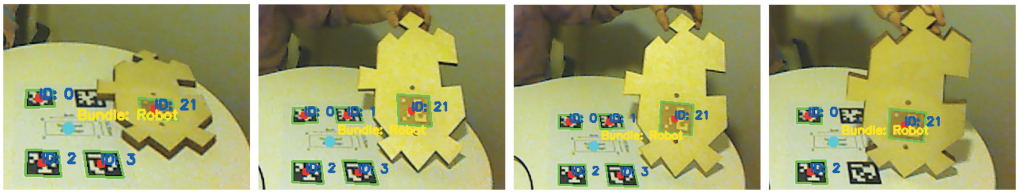

(a) 1 panel, 0° (b) 1 panel, 30° (c) 1 panel, 60° (d) 1 panel, 90°

(e) 2 panels (f) 3 panels (g) Misaligned (h) Mis. - Top (i) Mis. - Far

Figure 5. Testing panels, with and without a reference bundle. a-d show the movement of a single panel through 30° increments, allowing us to test the orientation accuracy of the pose estimation. e-f show adding panels, to test the alignment of secondary panels to the as-designed configuration. g-f shows experiments with camera distance and orientation on 2 deliberately misaligned panels.

3 RESULTS

For the majority of tests (Figure 5(a)-5(g)), the camera was setup on a stand 1.4m high and 0.7m horizontally away from the tag bundle, was placed on a 0.7m table, with almost exactly a metre from the camera to the base tag, meaning that the camera made a 45° angle with the base bundle. Maximum panel dimensions were measured using axis aligned bounding boxes, and found to be 31.4cm, 29.7cm and 25.8cm for panels 21, 28 and 48 respectively.

Table 1. Measurements of single panel angle experiment using panel 21.

Panel angle ()	Measured Angle ()	Angle error (%)	PCL ADD (cm)	ADD/Panel size (%)
0	1.7	∞	2.7	8.5
30	30.8	2.6	3.1	10.0
60	65.8	9.7	3.4	10.8
90	84.7	-5.9	2.0	6.5

In Table 1, the measurements of the panel being moved through 30° angles with respect to the base bundle are shown and the measured angle of the panel is compared. At lower angles, the measurement is extremely accurate, although at higher angles the angle deviates particularly at 60°. Since the 60° and 45° measurements have the same respective angle from the camera frame of 45, we surmise that this is due to the differing lighting conditions as the panel moves.

Additionally, the panel locations measured were compared to the pointcloud data using equation 1. In general according to the literature, ADD is deemed to show accuracy when its value is less than 10% of the objects maximum dimension, which is shown in the 0° and 90° case - this represents a misalignment of the pointcloud in the range of 2.0-3.4cm.

Table 2 shows the results of the tests in Figure 5(e)-5(f). It should be noted that there are some much higher errors here with relation to the pointcloud data, with nearly 25% ADD error indicating potential issues. However, for the comparison of as-designed to real locations, using panel 21 as a reference pose, the panels are within 2.1% pose accuracy.

Table 2. Adding extra panels and comparing to as-designed locations, using #21 as a ground truth.

Panel	Test	2 panel	3 panel
3*21 (reference)	ADD	Reference panel	
	PCL ADD (cm)	6.6	4.4
	PCL ADD (%)	21.1	13.9
4*28	ADD (cm)	0.6	0.6
	ADD (%)	1.9	2.1
	PCL ADD (cm)	2.4	2.8
	PCL ADD (%)	7.9	9.6
4*48	ADD		0.5
	ADD (%)		1.9
	PCL ADD (cm)		6.1
	PCL ADD (%)		23.8

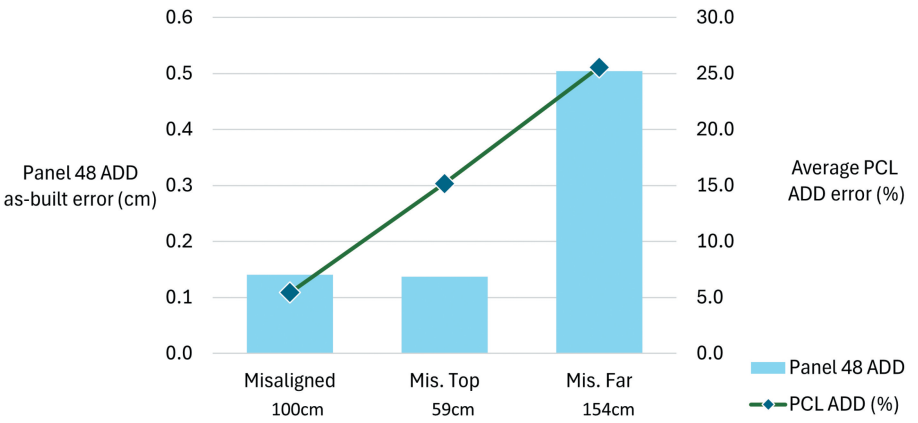

Figure 6. Comparing as-built error estimation, and PCL error over different distances.

Fig. 6 Shows the effect of changing location and orientation as depicted in Figure 5(g)-5(i). The same misalignment is maintained, and this is shown by the 0.35cm max variation in the as-designed to as-built ADD error comparison. It seems that the pointcloud is highly inaccurate now here, with the most accurate location observed at 1 metre away, and 50cm variation either way causes divergence from the Apriltag ground truth measurements.

4 DISCUSSION & CONCLUSIONS

A panel system is shown and a digital fabrication solution provided which provides maximum sized fiducial tags and manufacturing of geometrically complex components at low cost in timber. The system is fully bespoke, however, the dry stacking and friction/cantilevering stability of the structures is beneficial for disassembly purposes.

The use of a bundle of base tags to be placed at known locations from the robotic assembly agent allows the accurate understanding of the robot pose in relation to the built structure. Of particular utility here is the fact that the robot could be feasibly moved during assembly if online planning is used, as the camera's relative pose and the relative panel poses can be calculated live. Additional cameras could be integrated to provide a more comprehensive view of

the scene, so long as they have a view of at least one of the bundle tags, as shown by the accurate estimation of the partially obscured bundle in Figure 5.

The single panel experiments show a high angular estimation accuracy for the Apriltag system, allowing the measurement of architectural components poses. The availability of this data in realtime should improve the capabilities of robotic manipulators in the transfer and assembly of parametrically designed structures to real sites. Particularly, the feedback of live data is something that is often missing in CAD based robotics solutions which are generally uni-directional, plan-fire-forget systems, and fiducial tag systems are a useful and relatively straightforward solution for scene understanding.

The multiple panel assembly experiments show promising results again for measuring as-built accuracy, and highlight that such systems would be of aid in the placement of building components with high accuracy requirements into interlocking or otherwise constrained systems. Additionally, the use of multiple reference panels, as would be the case in the full panel system, would provide multiple estimates for placement location, allowing the programmer to gain a more accurate place location based on its neighbours.

The system demonstrates relatively high accuracy over different distances and orientations, however the pointcloud representations are unfortunately inaccurate throughout. This suggests a need for further calibration steps to align the pointcloud and image data, either spatially (extrinsic calibration) or time synchronisation. With that, additional accuracy improvements can be explored and integrated into a manufacturing cell for robotic assembly tests.

REFERENCES

Bradski, G. (2000). The OpenCV Library. Dr. Dobb's Journal of Software Tools. Braumann, J (2019). KUKA|prc.

Chen, J. (2016). Falcon. Food4Rhino.

Fischler, M. A. & R. C. Bolles (1981). Random sample consensus: A paradigm for model fitting with applications to image analysis and automated cartography. Commun. ACM 24 (6), 381–395.

Garcia-Castellanos, D. & U. Lombardo (2007). Poles of inaccessibility: A calculation algorithm for the remotest places on earth. Scottish Geographical Journal 123 (3), 227–233.

Hinterstoisser, S., V. Lepetit, S. Ilic, S. Holzer, G. Bradski, K. Konolige, & N. Navab (2013). Model Based Training, Detection and Pose Estimation of Texture-Less 3D Objects in Heavily Cluttered Scenes. In K. M. Lee, Y. Matsushita, J. M. Rehg, and Z. Hu (Eds.), Computer Vision – ACCV 2012, Berlin, Heidelberg, pp. 548–562. Springer.

Iturralde, K., J. Shen, & T. Bock (2023). AprilTag detection for building measurement. International Symposium on Automation and Robotics in Construction (ISARC) Proceedings 2023 Proceedings of the 40th ISARC, Chennai, India, 589–592.

Iuorio, O., S. Wilcock, & E. Korkis (2024). Design for Deconstruction Through Digital Fabrication of Thin Spatial Systems. In V. Ungureanu, L. Bragan¸ca, C. Baniotopoulos, and K. M. Abdalla (Eds.), 4th International Conferences"Coordinating Engineering for Sustainability and Resilience" & Midterm Conference of CircularB "Implementation of Circular Economy in the Built Environment", Cham, pp. 262–272. Springer Nature Switzerland.

Malyuta, D. (2017). Apriltag ros. AprilRobotics.

Malyuta, D. (2018). Guidance, Navigation, Control and Mission Logic for Quadrotor Full cycle Autonomy. Master's thesis, ETH Zurich.

Quigley, M., B. Gerkey, K. Conley, J. Faust, T. Foote, J. Leibs, E. Berger, R. Wheeler, & A. Ng (2009). Ros: an open-source robot operating system. In Proc. of the IEEE Intl. Conf. on Robotics and Automation (ICRA) Workshop on Open Source Robotics, Kobe, Japan.

Song, Y., R. Koeck, & S. Luo (2021). Review and analysis of augmented reality (AR) literature for digital fabrication in architecture. Automation in Construction 128, 103762.

Tafazzoli, M. (2022). Construction Automation and Sustainable Development, pp. 73–95. Cham: Springer International Publishing.

Vestartas, P. (2021). OpenNest - 2D polyline packing for fabrication such as laser or CNC cutting.

Wilcock, S., H. Fang, M. R. Dogar, & O. Iuorio (2024). Integrating R-funicularity, local stability and inter-panel constraint assessment for discrete timber shell construction design. Structures 64, 106592